

Table of Contents

<u>Number</u>	<u>Page</u>
<i>Supplementary Materials and Methods</i>	2-19
<i>Supplementary Figures</i>	
Supplementary Fig. 1. Biochemical assay for identifying MDMX inhibitors	20-21
Supplementary Fig. 2. Quality control for MDMX HTS	22-23
Supplementary Fig. 3. Cell-based assay characterization and results	24-25
Supplementary Fig. 4. Chemotype representation of HTS data	26-27
Supplementary Fig. 5. Thermostabilization assay for MDMX inhibitors	28-29
Supplementary Fig. 6. Characterization of SJ-134433 and SJ-044557	30-31
Supplementary Fig. 7 SJ-172550 cytotoxicity requires p53	32-33
Supplementary Fig. 8 SJ-172550 cytotoxicity in cultured cells	34-35
Supplementary Fig. 9 Binding of SJ-172550 to MDMX mutants	36-37
<i>Supplementary Table</i>	
Supplementary Table 1. Data on 11 validated hits from MDMX HTS	38

SUPPLEMENTAL MATERIALS AND METHODS

Plasmid constructs and protein production. The p53-binding domain of mouse and human MDMX (a.a. 1-185) and human MDM2 (a.a. 1-188) were amplified by PCR and cloned into the pGEX-4T1 plasmid. Recombinant GST-fusion proteins were prepared in BL21(DE3) *E. coli* cells. Briefly, cells (12-48 L) were grown in culture at 37 °C to an OD₆₀₀ of 0.6 and then induced with 1 mM isopropyl- β -D-thiogalactopyranoside (IPTG) at 16 °C for 16 h. The cells were lysed and sonicated in TST buffer containing 50 mM Tris (pH 7.5), 150 mM NaCl, and 0.05% Tween 20 freshly supplemented with 10 mM DTT, 1 mM PMSF, protease inhibitor (Roche # 1873580), and 10 mg/L lysozyme {Arnold, 2006 #4135}. The lysates were cleared by spinning at 100,000 $\times g$, and the supernatant was loaded onto a 5-ml GSTrap Fast-Flow column (GE Life Sciences). The column was washed extensively with cold PBS containing 0.1% NP-40, and the fusion protein was eluted with 50 mM Tris 8.0 containing 30 mM reduced glutathione. Subsequent purification included a Mono-Q column and a S200 gel filtration column. Peak fractions were combined and dialyzed against PBS (pH 7.6) containing 2 mM PMSF. For mass spectrometry analysis of the purified protein, we desalted the samples using a reverse-phase c4 or c8 Zip Tip (Millipore) and eluted them in 50% water (unbuffered), 50% acetonitrile, and 2% formic acid. The eluent was ionized by static nanospray using EconoTips (New Objective) on a Micromass LCT mass spectrometer using the positive mode. The resultant charge envelope was deconvoluted using the MaxEnt 1 algorithm of MassLynx V4.0 SP4 software. A mass error of 1 Da per 10,000 Da is permissible using this mass spectrometer.

Fluorescence polarization assays. Fluorescence polarization (FP) assays were conducted in assay buffer containing 10 mM Tris (pH 8.0), 42.5 mM NaCl, and 0.0125% Tween-20. The wild type p53 peptide (a.a. 15-29) was GSGSSQETFSDLWKLLEN and the mutant AAA-p53 peptide was GSGSSQETFADLAKLAPEN. The FP assays were carried out using 2.5 nM FITC-peptide (or 15 nM Texas Red) and 1 μ M MDM2-GST or MDMX-GST. For MDM2-p53 or MDMX-p53 inhibitor assays, small molecules were preincubated with the recombinant protein for 30 min. The labeled peptide was then added and incubated for 45 min. FP assays were conducted in 384-well black microplates (Corning Life Sciences). The FP FITC assays were analyzed using an EnVision Multilabel plate reader with a 480-nm excitation filter, a 535-nm static and polarized filter, and an FP FITC dichroic mirror. The G-factor was set to 0.8. The dissociation constants (K_d s) and inhibition constants (K_i s) were calculated by fitting the data to a single-site binding mode with variable slope [$Y = \text{Bottom} + (\text{Top} - \text{Bottom}) / (1 + 10^{[(\text{LogEC}_{50} - X) * \text{HillSlope}])}$] using GraphPad Prism software. The unlabeled competitor peptide and nutlin-3 were used as positive controls, and the alanine-substituted p53 peptide (AAA-p53) was used as a negative control. To minimize the possibility of false-positive caused by endogenous fluorescence from the compounds in the library, we also developed an FP assay with the Texas Red fluorophore. This assay was the same as that used for the FITC experiments, except the FP Texas Red assays were run using a 555-nm excitation filter, a 632-nm static and polarized filter, and an FP Texas Red FP dichroic mirror. The G-factor was set to 0.8.

Chemical library and high-throughput screening. The screening library consisted of 296,488 unique compounds (ChemDiv, ChemBridge, and Life Chemicals) arrayed individually at 10 mM in DMSO in 384-well polypropylene plates. The quality of compounds was assured by the vendor as 90% pure. HTS was carried out on a system developed by High Resolution Engineering with integrated plate incubators (Liconic). Plates were transferred from instrument to instrument by a Staübli T60 robot arm. Assay materials were dispensed in bulk by using Matrix Wellmates (Matrix Technologies). Compound plates were centrifuged in a Vspin plate centrifuge (Velocity11). All compound transfers were accomplished by using a 384-well pin tool with 10-nL hydrophobic surface-coated pins (V & P Scientific). These pins allowed for the delivery of 25 nL to achieve a final compound concentration of 10 μ M. The fluorescent signal was measured using an EnVision multilabel plate reader.

Immunostaining and BrdU experiments. Cells were treated with drugs for 20 h or exposed to 5 Gy ionizing radiation (IR) followed by a 4.5-h incubation in culture at 37 $^{\circ}$ C. After being fixed in 4% paraformaldehyde, cells were immunostained with anti-p53 (DO-1, Santa Cruz #sc-126) or anti-caspase-3 (BD Pharmingen #557035) antibodies followed by species-specific secondary antibodies. To label S-phase cells, we added 10 μ M BrdU to the culture medium 1 h before collection. BrdU incorporation was analyzed using the cell proliferation kit (GE Life Sciences #RPN20). Bright-field and single-cell fluorescent images were obtained using a Zeiss Axioplan-2 fluorescent microscope with the Zeiss AxioCam digital camera. Specific protocols can be found at: <http://www.stjude.org/dyer> {Laurie, 2006 #2557}.

Protein preparation for Biacore/isothermal titration calorimetry. Human and mouse MDMX (a.a. 23-111) were cloned into a pHisDuet vector containing a 6× His-tag and TEV cleavage site. The proteins were expressed in *E. coli* BL21(DE3) RIL cells as follows. After inoculation, the cells were grown at 37° C and induced at OD600 between 0.6 and 0.8 with 0.6 mM IPTG. Upon induction, the temperature was shifted to 16 °C, and the cells were incubated overnight. Cell pellets were resuspended in 1 × PBS (pH 7.6), 10 mM imidazole, and 1 mM BME and lysed by sonication. MDMX was purified by Ni²⁺-affinity chromatography (His-Select Affinity Gel, Sigma) at 4 °C. Following affinity purification, MDMX was cleaved/dialyzed overnight in a solution of 50 mM Tris (pH 8.8), 200 mM NaCl, and 10 mM DTT. TEV was added at a 1:40 ratio based on the concentration determination by the Bradford protein assay. Following cleavage/dialysis, MDMX was further purified by size-exclusion chromatography using an SD75 column (GE Healthcare) at 4 °C. Purified MDMX was aliquoted, flash frozen in liquid nitrogen, and stored at –80 °C. Intact mass spectrometry on the purified protein generated a predominant peak corresponding to a mass of 10,292.5 Da (calculated mass, 10,293.1 Da) for human MDMX and a mass of 10,189.8 Da (calculated mass 10,189.9 Da) for mouse MdmX. Prior to ITC, proteins were dialyzed to remove DTT from the buffer, and 1 mM BME was used as the reducing agent. ITC experiments were conducted in an ITC200 (MicroCal). For Biacore studies, human and mouse MDMX (a.a. 1-185) and human MDM2, (a.a. 1-188) were produced and purified, as described above.

SDS-PAGE, silver staining, and immunoblotting. *E. coli* lysates and purified fractions were separated on 10% SDS-PAGE gels and stained with silver using the Pierce

SilverSNAP Stain Kit II according to the manufacturer's instructions. For immunoblotting, the proteins were separated by SDS-PAGE and transferred to nitrocellulose membranes (Invitrogen #IB3010-01) with the Invitrogen iBlot dry blotting system (#IB1001). Membranes were incubated with corresponding primary antibodies followed by IR Dye-labeled secondary antibodies; both were diluted in Odyssey blocking buffer (LI-COR #927-40000). Signals were detected with an Odyssey infrared imaging system (LI-COR) at 680 and 800 nm. Antibodies used for immunoblotting included anti-GST: goat polyclonal (abcam #ab6613), anti-GAPDH: mouse monoclonal 6C5 (abcam #ab8245), and rabbit polyclonal (abcam #ab8485), anti- β -Actin: rabbit polyclonal (abcam #ab8227), goat-anti-rabbit IgG (IRDye 680, LI-COR #926-32223, Red), and goat-anti-mouse IgG (IRDye 800CW, LI-COR #926-32210, green).

Peptide synthesis and modifications. The p53 peptide ligands were synthesized on a Rainin Symphony Multiplex 12-column peptide synthesizer. The sequence of the p53 peptide was GSGSSQETFSDLWKLLPEN, and the alanine-substituted negative control peptide (AAA-p53) was GSGSSQETFADLAKLAPEN. The FITC and Texas Red labels were added to the amino termini according to the manufacturers' instructions (Molecular Probes: Amine Reactive Probes) and purified using reverse-phase HPLC on Xterra C18 39 \times 50-mm columns with a linear gradient of 100% (0.01% TFA in water) to 20% (0.01% TFA in water) and 80% acetonitrile over 30 min and a flow rate of 20 mL/min. Quality control was carried out by HPLC-ESMS resulting in peptides with a purity greater than 98%. Because the p53 peptide contained lysine, the low pH and reaction time were important to ensure labeling at a single site. Full conversion was achieved after 4 h, and

the crude material was purified using the Parallax Flex HPLC System. For the AlphaScreen, the following N-terminal biotin-linked peptides were investigated: GSGSSQETFSDLWKLLPEN with PEG11 for MDMX or no linker for MDM2 between the peptide and biotin {Lu, 2006 #2525}. For BiaCore experiments, peptide concentrations were confirmed by the AAA Service Laboratory.

Cell culture experiments. Weri1 human retinoblastoma cells were obtained from the American Type Culture Collection and maintained in culture in RPMI with 10% fetal calf serum supplemented with penicillin, streptomycin, and *L*-glutamine. The SJmRbl-8 mouse retinoblastoma cell line was cloned from a retinoblastoma tumor removed from a *Chx10-Cre;Rb^{+Lox};p107^{-/-};p53^{Lox/Lox}* mouse. Weri1 and SJmRbl-8 cells were plated in white 384-well plates at a density of 100,000 cells/mL and 25,000 cells/ml, respectively. The final volume was 25 μ L. Compounds dissolved in DMSO were added to the cells by using the pin tool, and the final concentration of DMSO was 0.6%. As a negative control, cells were incubated in the presence of 0.6% DMSO. As positive controls, we used nutlin-3a, vincristine, and staurosporine at various concentrations. After a 72-h incubation, cells were lysed and ATP was measured by the CellTiter-Glo Luminescent Assay Kit (Promega #G7570). Plates were mixed on an orbital shaker at 600 rpm for 2 min and incubated at room temperature for an additional 10 min. The luminescent signal was quantified using the Envision Multilabel Plate Reader (PerkinElmer). Each experiment was performed in triplicate. For the dose-response curves, the data were fit using CurveFit NCGC software (NIH Chemical Genomics Center).

Biacore measurement of the binding constant. Binding experiments were performed at 25 °C using a BIACORE T100 (GE Healthcare) surface plasmon resonance (SPR) instrument. Anti-GST antibodies (GE Healthcare) were covalently attached to a carboxymethyl dextran-coated gold surface (CM5 Chip; GE Healthcare). The carboxymethyl groups were activated with *N*-ethyl-*N'*-(3-dimethylaminopropyl) carbodiimide (EDC) and *N*-hydroxysuccinimide (NHS). Anti-GST antibodies were attached at pH 5.0 in 10 mM sodium acetate. Any remaining reactive sites were blocked by reaction with ethanolamine. Antibodies were immobilized to levels of approximately 8600 to 11800 RU in each flow cell.

The binding of p53 peptides to MDMX or MDM2 was monitored at a flow rate of 50 μ L/min. GST-MDMX or GST-MDM2 were captured to levels of approximately 2200 to 2500 RU. GST was captured on the reference surface to account for nonspecific binding to the GST tag. Wild-type and mutant p53 peptides were prepared as a 2-fold serial dilution (61 nM-3.9 μ M) in 10 mM Tris (pH 7.6), 200 mM NaCl, 0.1 mg/mL bovine serum albumin, and 0.005% Tween20. To account for injection artifacts, we recorded a series of sensorgrams throughout the experiment after injecting only buffer (blank injections).

The peptides dissociated completely from the chip surfaces, eliminating the need for a regeneration step. Data reported are the differences in SPR signal between the flow cells containing GST-MDMX or GST-MDM2 and the reference cell containing GST only. Additional instrumental contributions to the signal were removed by subtraction of the average signal of the blank injections from the reference-subtracted signal. Triplicate

injections were made, and the data were analyzed by equilibrium-affinity analysis using Scrubber 2 software (Version 2.0b, BioLogic Software).

Isothermal titration calorimetry. Protein peptide interactions were quantitated at 25 °C in a MicroCal ITC 200 calorimeter. The experiment involved the injection of 11 aliquots of 250 μ M p53 peptide (acetyl-TPGPADAMHRKHLQE-NH₂). The first injection volume was 0.3 μ L, and the remaining were 3.75 μ L into the cell with 20 μ M human MDMX²³⁻¹¹¹. Solid peptide was dissolved in protein-dialyzed buffer containing 25 mM Tris (pH 8.8), 200 mM NaCl, and 1 mM BME. The integrated interaction heat values were analyzed using Origin software (v7.0552, MicroCal) to determine binding affinity, stoichiometry, and thermodynamic parameters.

Dose-response experiments. DMSO was added to columns 3 through 20 of a 384-well plate (Biomek FXP, Beckman Coulter). Then 10-mM compound stocks were transferred from the source plates to the first or second column of the plate. Each plate contained 32 compounds. Serial dilutions (1:3) were made using a Tecan Freedom Evo 150, with 10 total dilutions for each compound. A separate control plate was made using column 21 through 24 with similar dilutions of positive controls (i.e., nutlin-3a or peptide) or negative controls (i.e., DMSO or AAA-p53). One control plate was used for each screening run. Plates were centrifuged at 4,000 rpm for 2 min before use. Analysis of the dose-response data was carried out using RISE software. Detailed protocols can be found at <http://hc-pp1.stjude.org:9944/>, and all screening results can be found at <http://hc-pp1.stjude.org:9944/assayreporter/>.

Cooperativity Assay. Weri1 cells were plated at a density of 100,000 cells/mL on 384-well plates (Corning #8804BC); a Wellmate machine (Matrix Technologies) was used to insert 2500 cells/25 μ L per well. The cells were then treated with nutlin-3a alone, MDMX inhibitor compound alone, or the combination of nutlin-3a and the compound for 72 h at 37 °C. Compounds were made into 10-mM stocks in DMSO, and the molar ratios of nutlin-3a:MDMX inhibitor compounds were 5:1, 3:1, 1:1, or 1:3. The highest final drug concentration used was 60 μ M for total compound concentration, and 1:2 dilutions were used until the drug concentration reached 0.003662 μ M. After the incubation, cells were lysed and ATP levels were measured, as described above. Dose-response curves were fitted to a single-site binding mode with variable slope [$Y = \text{Bottom} + (\text{Top} - \text{Bottom}) / (1 + 10^{((\text{Log}_{\text{EC}} - X) * \text{HillSlope}))}$)] by using GraphPad Prism software. LC_{50} s (and LC_{90} s) were calculated accordingly and plotted with Microsoft EXCEL. The error bars represent the standard deviation from 2 independent experiments.

Coimmunoprecipitation. The antibodies for coimmunoprecipitation (co-IP) were anti-p53 FL393 rabbit polyclonal IgG (Santa Cruz sc-6243), DO-1 mouse monoclonal IgG (Santa Cruz sc-126), anti-MDMX: D19 mouse monoclonal IgG (Santa Cruz sc-14738), anti-MDM2: SMP14 mouse monoclonal antibody (Santa Cruz sc-965), anti-Flag OctAprobe (D-8) (Santa Cruz sc-807), and anti-HA 12CA5 monoclonal (Abgent AM1008a). Cells were lysed with TGN buffer containing 20 mM Tris (pH 7.5), 150 mM NaCl, 1% Tween-20, and 0.2% NP-40 freshly supplemented with 50 mM NaF and protease inhibitors (Roche #11836153001). Lysates were cleared and subjected to co-IP

with corresponding antibodies followed by protein A/G agarose separation (CalBiochem IP#10). Samples were washed with an excessive amount of TGN buffer and then applied to an SDS-PAGE gel followed by Western blotting.

Isothermal denaturation assay. The ITD measurements were performed with a RT-PCR instrument (Applied Biosystems 7900HT) equipped with a 384-well probe using SYBR detection (495/537). The program used started at 25 °C for 30 s; increment: 25 °C for 0.01 s and 26 °C for 0.55 s with 50 repeats. The autoincrement was 1 °C with a ramp rate of 100%. The final concentrations were 0.125 mg/mL MDMX, 30 µM compound, and 5× SYPRO orange (Invitrogen) in a buffer consisting of 10 mM TRIS (pH 8.0) and 25 mM NaCl. The final volume was 20 µL for each well using 384 ABI PRISM™ plates (Applied Biosystems). The data were exported and evaluated using PrismPad. The melting temperatures (T_m) were obtained by fitting the data to an equation (sigmoidal dose-response (variable slope) or 4 parameter logistic equation): $[Y = \text{bottom} + (\text{top} - \text{bottom}) / (1 + 10^{((\log IC_{50} - X) * \text{HillSlope}))}]$, where X is the logarithm of temperature, and Y is the fluorescence intensity. The experiment was carried out in triplicate, and the T_m values are given as the mean values with a 95% confidence interval.

Redox assay. Redox activity of all hits was determined using a high-throughput assay based on the detection of molecules capable of reducing resazurin (#R7017, Sigma) to resorufin. This method has been used previously to identify compounds acting via redox mechanisms in a wide range of high-throughput settings {Lor, 2007 #4277}. Briefly, 25 µL assay solution containing 5 µM resazurin, 50 mM HEPES, 50 mM NaCl (pH 7.5), and

50 μM DTT was added to a black 384-well polystyrene plate (#3573, Corning) using a Matrix WellMate (Thermo Fisher Scientific). Test compounds were added by pin transfer using 10 nl hydrophobic-coated pins (FP1CS10H, V&P Scientific) to a final concentration of 10 μM . A pyrimidotirazinedione-containing compound (10 μM D052-0147, ChemDiv Inc.) was used as a positive control, and DMSO was used as a negative control. Test plates were incubated in the dark at room temperature for 60 min, and fluorescence intensity was read on an Envision plate reader (PerkinElmer (Excitation, 560 nm; Emission, 590 nm)). Each compound was read in quadruplicate, and the signals were averaged to generate relative activity levels. Compounds that differed significantly from DMSO levels, as determined by RISE 3.0 software, were scored as being potentially redox active.

Permeability. Parallel artificial membrane permeability assay (PAMPA) was conducted by Biomek FX lab automation workstation (Beckman Coulter) and PAMPA evolution 96 command software (pION). Briefly, 3 μL of 10 mM test compound stock was mixed with 597 μL system solution buffer (SSB, pH 7.4; pION) to make a diluted test compound. A 150- μL sample of diluted test compound was transferred to a UV plate (pION), and the UV spectrum (250-500 nm) was read as the reference plate. The membrane on preloaded PAMPA sandwich (pION) was painted with 4 μL GIT lipid (pION). The acceptor chamber was then filled with 200 μL acceptor solution buffer (pION), and the donor chamber was filled with 180 μL diluted test compound. The PAMPA sandwich was assembled, placed on the Gut-box (pION), and stirred for 30 min. An aqueous boundary layer was set to 40 μm for stirring. The UV spectrum (250-500 nm) of the donor and the

acceptor were read. The permeability coefficient was calculated using PAMPA evolution 96 command software (pION) based on the area under the curve (AUC) of the reference plate, the donor plate, and the acceptor plate. All compounds were tested in triplicate.

Solubility. Solubility assay was carried out on Biomek FX lab automation workstation (Beckman Coulter) using μ SOL Evolution software (pION). Briefly, 10 μ L of 10 mM compound stock was added to 190 μ L 1-propanol to make a reference stock plate. A 5- μ L sample from this reference stock plate was mixed with 70 μ L 1-propanol and 75 μ L SSB (pH 7.4) to make the reference plate. The UV spectrum (250-500 nm) of the reference plate was read. A 6- μ L sample of 10 mM test compound stock was added to 600 μ L SSB in a 96-well storage plate and mixed. The storage plate was sealed and incubated at room temperature for 18 h. The suspension was then filtered through a 96-well filter plate (pION). The filtrate (75 μ L) was mixed with an equal volume of 1-propanol to make the sample plate, and the UV spectrum of the sample plate was read. Calculation was carried out by μ SOL Evolution software based on the AUC of the UV spectrum of the sample and reference plates. All compounds were tested in triplicate.

Mass spectrometry. Each protein solution (1 μ L) was spotted in triplicate on a stainless steel MALDI target with 1 μ L of sinapinic acid (20 mg/mL in 50% acetonitrile, 0.1% trifluoroacetic acid in water) and mixed by pipet. Spots were allowed to air dry and crystals to form. Spectra were acquired in an automated manner on a Bruker Autoflex II mass spectrometer (Bruker Daltonics) equipped with a SmartBeam Laser (Nd:YAG, 355 nm) operated at 100 Hz. Spectra were acquired in linear positive ionization mode. An

accelerating voltage (20 kV) was used with an extraction voltage (18.40 kV) and an Einzel lens voltage (6.00 kV). Delayed extraction was optimized for resolution at 50 kDa. Each spectrum was the sum of 2000 laser shots in increments of 100 shots, with the laser position within a sample spot moved between each successive laser firing. All spectra were preprocessed using ProTS software (Biodesix, Inc.). Preprocessing included baseline correction, noise estimation, and normalization to total ion current. Replicates from the same sample were averaged, and the averages were plotted using Origin software (OriginLab Corporation).

Cooperativity assays/isobologram. Weri1 cells were plated at 100,000 cells/mL on 384-well plates (Corning) by using a Wellmate machine (Matrix Technologies). They were then treated with nutlin-3a alone, SJ-172550 alone, or a combination of both for 72 h at 37 °C. Drugs were made into 10-mM stocks in DMSO, and the molar ratios of nutlin-3a: SJ-172550 used were 1:1, 1:5, 1:10, or 1:20 based on their LC_{50} . The highest final drug concentration used was 60 μ M for total drugs, and 1:2 dilutions were used until drug concentration reached 0.003662 μ M. After the incubation, cells were lysed, and ATP levels were measured. Dose-response curves were fitted to a single-site binding mode with variable slope [$Y = \text{Bottom} + (\text{Top} - \text{Bottom}) / (1 + 10^{((\text{LogEC}_{50} - X) * \text{HillSlope}))}$] by using GraphPad Prism software. LC_{50} s were calculated accordingly, and error bars represent the standard deviation from 2 independent experiments.

Western blot and immunoprecipitation analyses. Western blotting and immunoprecipitation were performed as described (27, 35, 36). Briefly, cells were either

mock-treated or treated with 20 μ M SJ-172550 for 20 h and then lysed in Giordano(150) buffer containing 50 mM Tris (pH 7.4), 150 mM NaCl, 0.1% Triton X-100, and 5 mM EDTA, with 10% glycerol and protease inhibitors. In the lysis buffer of the SJ-172550–treated cells, SJ-172550 was also included to prevent dissolution and reassociation of MDM2-p53 and MDMX-p53 binding in the lysate. The immunoprecipitations were performed overnight at 4 °C. Antibodies used for Western blotting or immunoprecipitations were as follows: anti-p53 FL393 (#sc6243), anti-p53 DO-1 (#sc126), and anti-MDM2 SMP14 (#sc965) from Santa Cruz; anti-p53 AB-7, anti-MDMX (Bethyl # BL1258), anti-MDMX (MX-82, Sigma #M0445), anti-MDM2 (4B2, gift from Dr. A. Levine), anti-HAUSP, anti-GAPDH: mouse monoclonal 6C5 (abcam #ab8245), rabbit polyclonal (abcam #ab8485), and Anti- β -actin: rabbit polyclonal (abcam #ab8227).

Real-time PCR. Real-time PCR reactions were set up by Eppendorf epMotion automated pipetting system and were performed using an Eppendorf real-time RT-PCR machine. RNA was prepared using TRIzol, and cDNA was synthesized using the SuperScript system (Invitrogen). TaqMan probes were synthesized with 5'-FAM and 3'-BHQ. Samples were analyzed in duplicate and normalized to *GAPDH* or *GPII* expression levels. Primers and probes were designed using Primer Express[®] software (Applied Biosystems).

Methods and Rationale for Selection of 7 Mutants in the p53 Binding Pocket of MDMX to Study Binding to SJ-172550, p53 peptide and nutlin-3a

Docking results were obtained using both the AutoDock suite(1) and Scigress Explorer version 7.7. The Autodock results were obtained using the default Lamarckian genetic algorithm. An initial population size of 300 was used with 40,000 generations and 5×10^7 energy evaluations per docking run. Mutation rates of 0.02, 0.05, and 0.10 were used with crossover rates of 0.80 and 0.85 for a total of six independent docking runs with 30 passes each. The elitism factor was set to 7 in each case.

Docking runs with Scigress Explorer employed a potential of mean force (PMF) algorithm with an initial population size of 50, elitism 7, 60,000 generations, crossover 0.80 and mutation 0.20. Docked structures obtained from Scigress were then reoptimized using the MOZYME algorithm with the PM3 Hamiltonian and the COSMO solvation model to obtain final structures.

Relative enthalpies of formation of the bound state versus the free systems for wild type versus mutant protein were determined by mutation of the relevant residue in the docked structure obtained with Scigress Explorer. The mutant residues were then optimized using the MM3 force field while holding the remainder of the structure fixed. The entire structure was reoptimized using the PM3/COSMO procedure described above followed by single point energy calculations of the apo protein structure and the bound conformation of the ligand in the absence of MDMX.

Cluster analysis of the Autodock results for SJ172550 against the 3DAB crystal structure revealed two clusters with predicted K_i values of 8.66 and 60.59 μM , respectively. The higher-energy cluster contained 10 structures compared to 72 in the lowest-energy cluster. Results from the docking using Scigress were in agreement with those from the lowest-energy Autodock cluster.

The primary binding site showed close interactions between the ligand and residues HIS54, GLN58, MET61 and TYR66 (see Figure 9). Based on visual inspection, thirty-eight point mutations were proposed in an attempt to disrupt the binding of SJ172550 while preserving the binding of the native peptide segment from p53. Relative enthalpies of formation were used to rank the considered mutants at each position and then selected based energetic, structural and chemical considerations.

Sequence alignments of the MDMX (3DAB) and MDM2 (3GO3) sequences suggested two mutations, H54F and M53L, to create a binding pocket with structural similarity to the binding region in MDM2 within the MDMX scaffold. Two other mutants, M61I and Y66I, were chosen based on their high calculated relative enthalpies and their potential to disrupt the ligand binding through steric clashes. Similarly, the Q58D mutant appeared energetically unfavorable and introduced a charge-charge interaction with the halogen moiety in the ligand. The Q71K represents a dramatic change to the protein structure without introducing large deformations of the backbone which would likely lead to steric clashes in the binding site.

The final suggested mutation is a quadruple mutant (P95H, S96R, P97K, and R103Y) intended to alter the helix near the secondary binding site to locally mimic the MDM2 structure. Strongest interactions from the docking results were seen with GLN26, VAL27, VAL49, LYS50, MET53, TYR99, LEU102, ARG103, LEU106 and THR108.

MOZYME/PM3 +

COSMO Geometry

(kcal/mol)

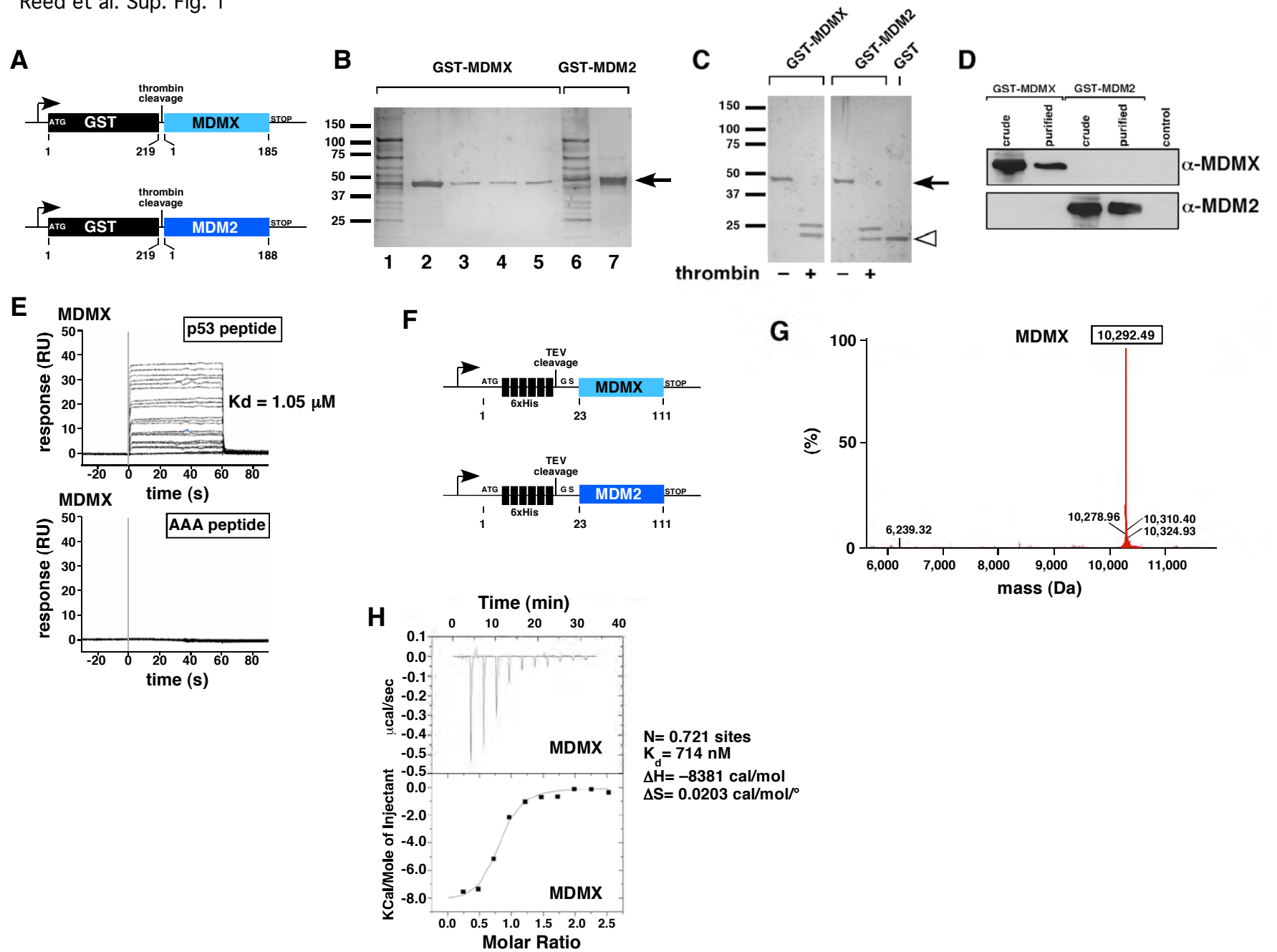
Mutant	Relative to	
	$\Delta\Delta H_f$	Wild Type
H54A	86.537	69.203
H54D	105.318	50.423
H54E	83.597	72.144
H54F	85.801	69.940
H54F_Q71H	82.303	73.437
H54G	101.808	53.932
H54I	93.785	61.955
H54L	80.226	75.514
H54M	83.753	71.987
H54N	81.413	74.328
H54P	97.483	58.258
H54S	96.771	58.970
H54Y	83.758	71.982
M61D	102.757	52.984
M61G	96.852	58.889
M61I	88.363	67.377
M61L	97.538	58.203
M61N	102.717	53.024
M61P	93.609	62.132
M61T	98.957	56.784
M61V	96.242	59.499
3DAB (Wild Type)	155.740	0.000
Q58A	88.756	66.985
Q58D	80.173	75.567

Q58E	96.585	59.156
Q58G	88.874	66.866
Q58I	90.721	65.020
Q58L	89.366	66.374
Q58P	103.571	52.169
Q58S	90.628	65.112
Q58T	101.610	54.130
Q58V	106.071	49.669
Q71H	83.486	72.255
Y66A	98.813	56.928
Y66G	95.338	60.402
Y66I	92.450	63.290
Y66L	96.813	58.927
Y66P	93.770	61.971
Y66V	105.400	50.341

SUPPLEMENTAL FIGURES

Supplemental Figure 1. Biochemical assays for high-throughput screening to identify MDMX inhibitors. (A) Map of the expression vector *pGEX-4T1* containing human MDMX (a.a. 1-185) and human MDM2 (a.a. 1-188). Recombinant GST-fusion proteins were prepared in BL21(DE3) *E. coli* cells and purified. The purity, size, and identity of proteins were confirmed with silver staining (B), thrombin cleavage (C), and immunoblot analyses (D). (E) MDMX interaction with wild-type p53 peptide but not AAA-p53 was confirmed with Biacore studies, and the K_d value was consistent with results from our FP assays. (F) Constructs of recombinant MDMX (a.a. 23-111) and MDM2 (a.a. 23-111) used for ITC measurements. (G) Mass spectroscopic confirmation of the purity of GST-MDMX²³⁻¹¹¹. (H) ITC measurement of MDMX binding to p53 peptide. The K_d was consistent with results from Biacore and FP assays.

Reed et al. Sup. Fig. 1



Supplemental Figure 2. Quality control measurements for MdmX high-throughput

screens. (A) Each plate in the HTS had a series of replicate dose-response wells with unlabeled p53 peptide as a positive control. The distribution of EC₅₀ values for reference peptide was stable across the screen. Each day of screening is marked with a yellow line.

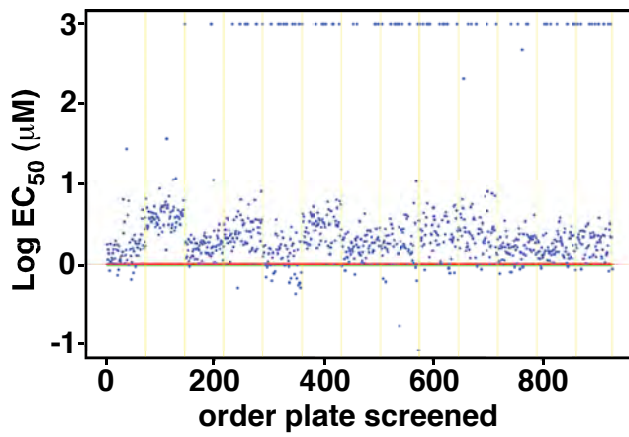
(B) Distribution of initial hits per plate. Hits are defined as activity greater than 70% for the primary screen. The red plot indicates the smoothed average, suggesting that the average hit percentage was approximately 1% to 2% across the assay. (C) Box plots for the primary screen in which the green plot represents the positive controls; the red plot represents the negative controls; and the gray plot represents the variable compounds.

There was drift in the raw assay endpoint each day, but the separation between positive and negative controls remained relatively stable. (D) Distribution of z' over the assay.

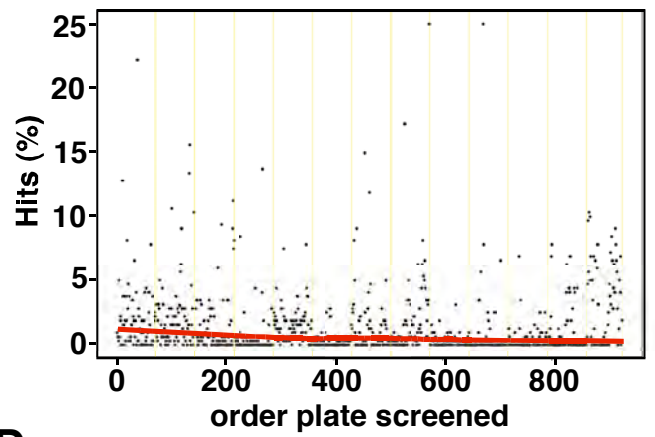
The red line is the smoothed average. (E) Average well activities over the entire assay for all plates from the primary screen were normalized to the z-score. Positive and negative controls are in columns 1, 2, 13, and 14. (F) Distribution of the total number of hits per well for the entire assay. There was minimal bias across the plate, in terms of hits or well activity across the screen.

Reed et al. Sup. Fig. 2

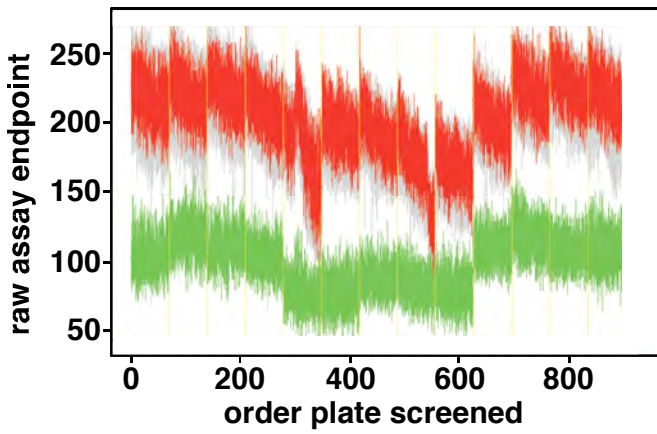
A



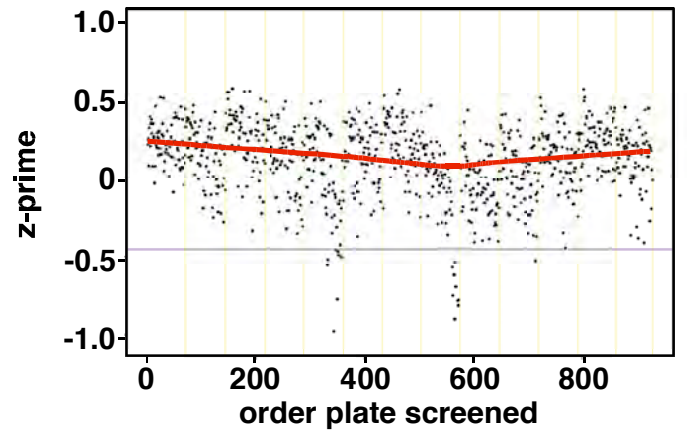
B



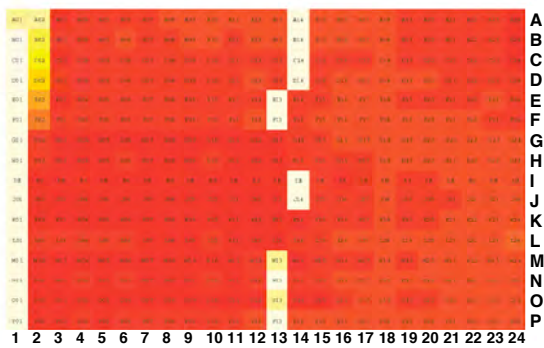
C



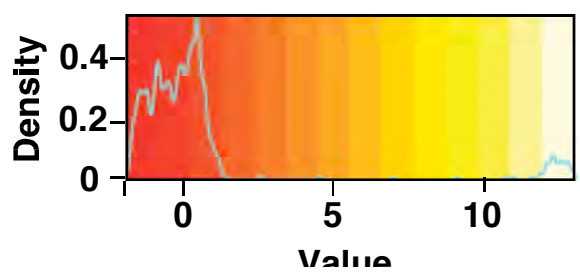
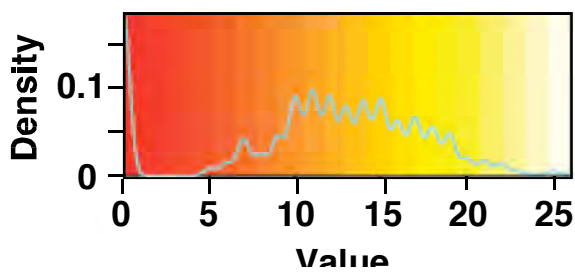
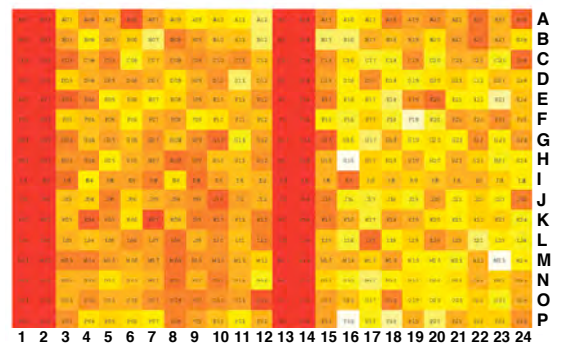
D



E

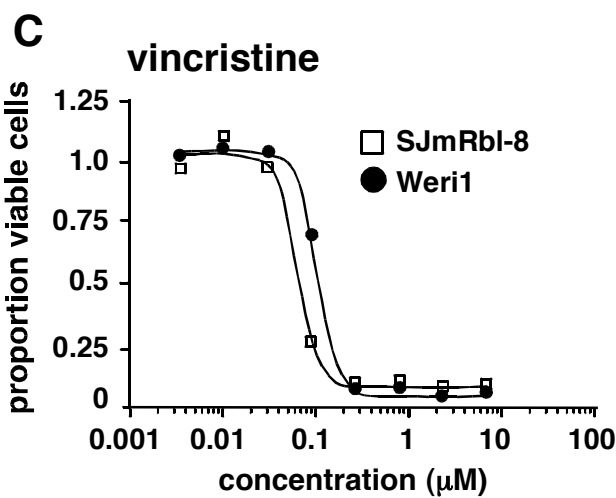
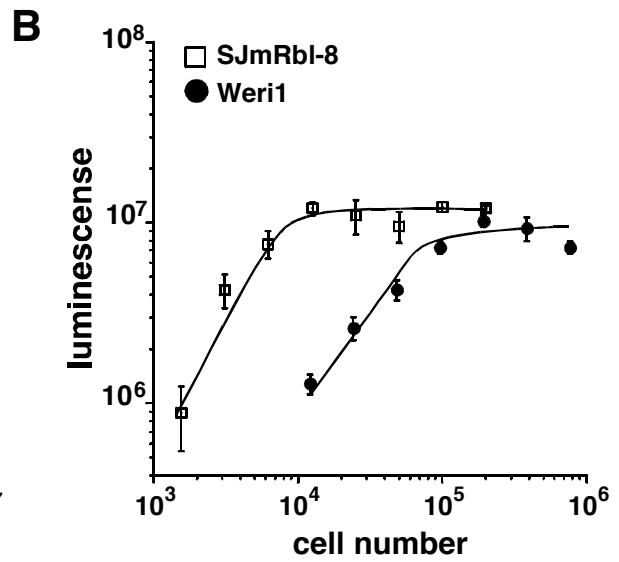
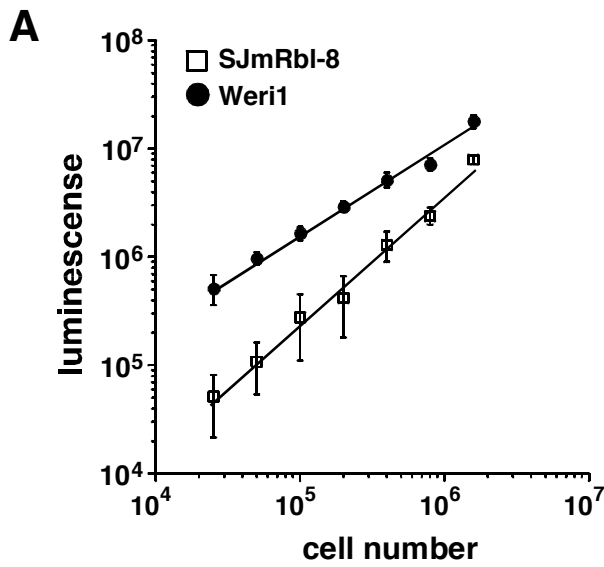


F

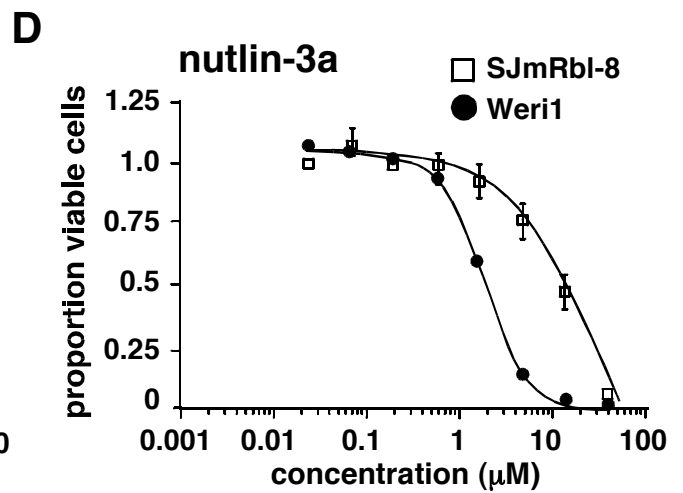


Supplemental Figure 3. Cell-based assay characterization and results from the high-

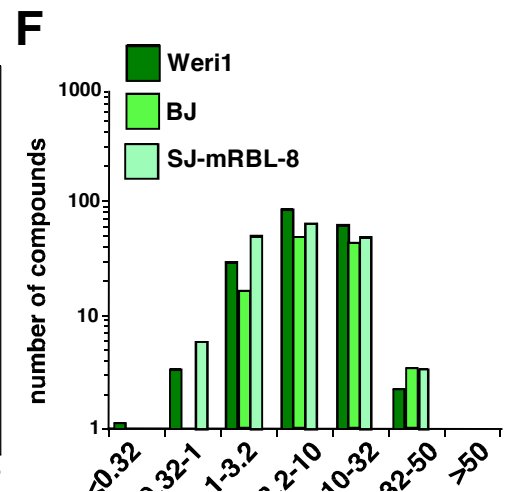
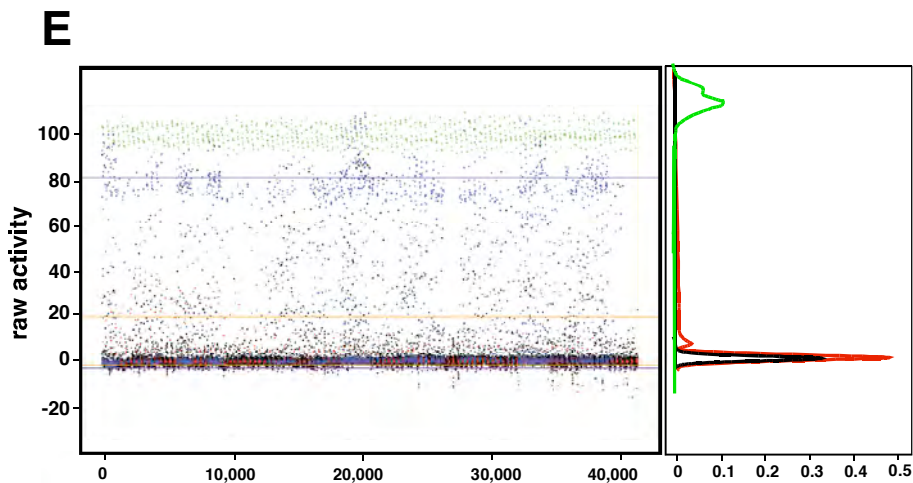
throughput screens. (A) In the first experiment, the range of viability of Weri1 and SJmRbl-8 cells plated at various densities was determined. The indicated number of cells was incubated and read immediately on an Envision plate reader. (B) In the second experiment, Weri1 and SJmRbl-8 cells were plated at different densities (as indicated) and grown for 72 h to determine if the cells would outgrow the linear range of the CellTiter Glo assay. From these 2 experiments, we determined that the optimal plating density for Weri1 cells was 1×10^5 cells/mL and for SJmRbl-8 cells was 2.5×10^4 cells/mL for the 72-h assay. Weri1 and SJmRbl-8 cells were incubated in different concentrations of vincristine (C) and nutlin-3a (D), and cytotoxicity was measured using the CellTiter-Glo assay. Vincristine showed no cell-type specificity, but nutlin-3a selectively killed the Weri1 cells, which expressed wild-type p53. (E) Scatterplot of HTS of MDMX inhibitors for Weri1 cytotoxicity. The red plot indicates minimum cytotoxicity from the negative control DMSO; the green plot represents the maximum cytotoxicity from the positive control vincristine; and the black plot represents the compounds that did not exhibit activity in cell growth inhibition. The blue data points are the compounds that showed various levels of cytotoxicity and were selected for further analysis. The density plot illustrates the clear separation of the positive and negative control samples across the entire screen. (F) The EC_{50} was calculated for each cell line and each compound in the dose response for the 1,152 compounds that were selected from the biochemical analysis of MDMX inhibitors. This histogram highlights the number of compounds with EC_{50} s in the indicated range for each cell line.



	Weri1	SjmRbl-8
EC_{50}	0.11 μM	0.06 μM



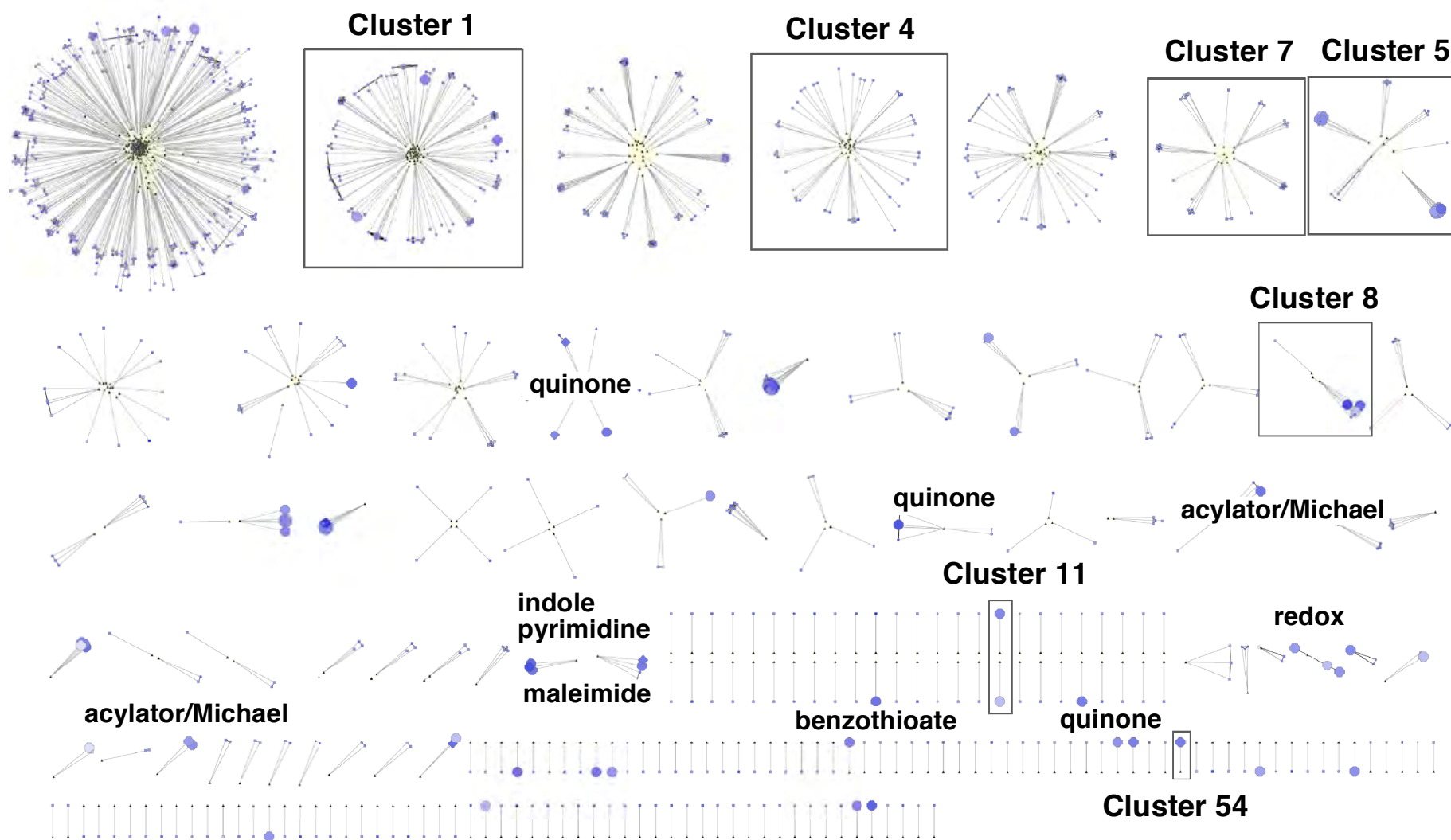
	Weri1	SjmRbl-8
EC_{50}	2.67 μM	71.4 μM



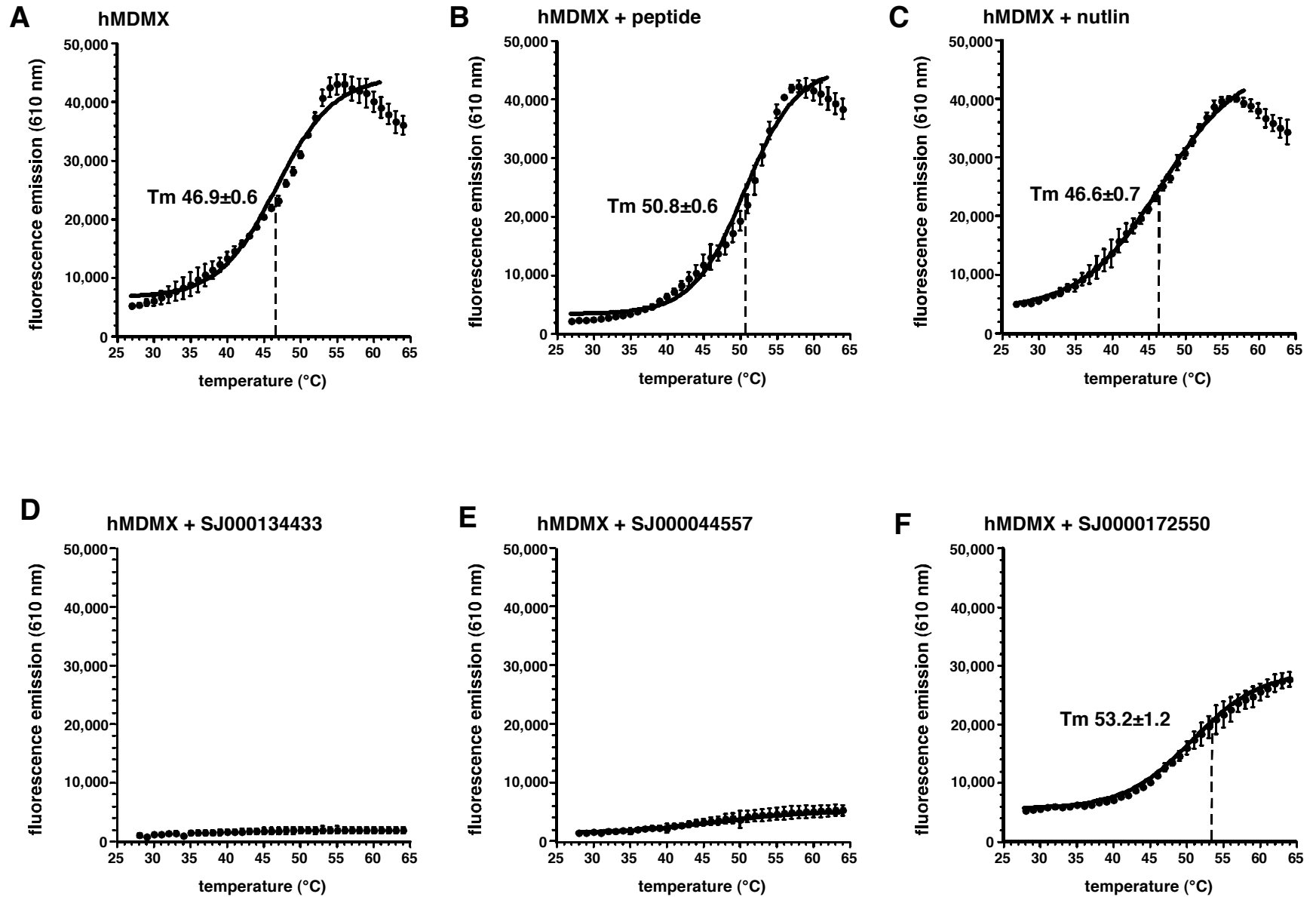
Supplemental Figure 4. Chemotype representation of the high-throughput screen

data. The chemical structures shown are the Murcko scaffolds. The black triangles are compounds related to that Murcko scaffold, and each gray line from those triangles represents a compound in the plate. The shading of the circles for each compound is related to its binding constant for MDMX, and the size reflects the selective cytotoxicity for retinoblastoma cells versus BJ cells. Large, dark blue circles are those with low binding constants for MDMX and selective cytotoxicity for retinoblastoma cells versus BJ cells. Clusters 1, 4, 5, 7, 8, 11, and 54 were selected for further analysis.

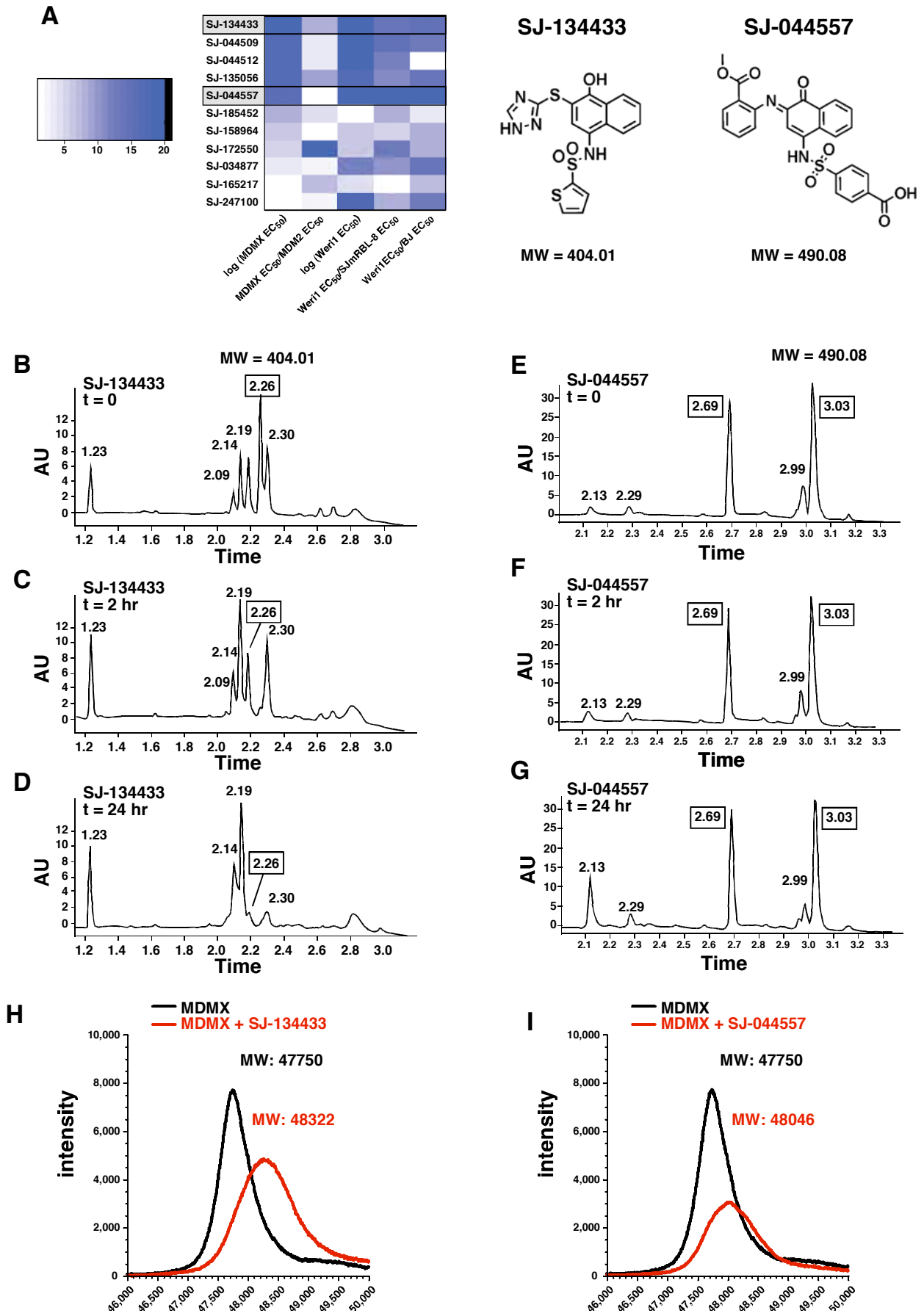
Reed et al. Sup. Fig. 4



Supplemental Figure 5. Thermostabilization assay for MDMX inhibitors. (A) The melting temperature (T_m) of GST-MDMX¹⁻¹⁸⁵ was 46.9 ± 0.6 °C. This measure shifted to 50.8 ± 0.6 °C in the presence of p53 peptide (B). Nutlin-3a did not thermostabilize MDMX (C). Neither SJ-134433 (D) nor SJ-044557 (E) exhibited a thermal shift; in fact, it appeared that the protein was disrupted or inactivated in these assays. (F) SJ-172550 increased the thermal stability of MDMX, as indicated by the shift in T_m to 53.2 ± 1.2 °C.

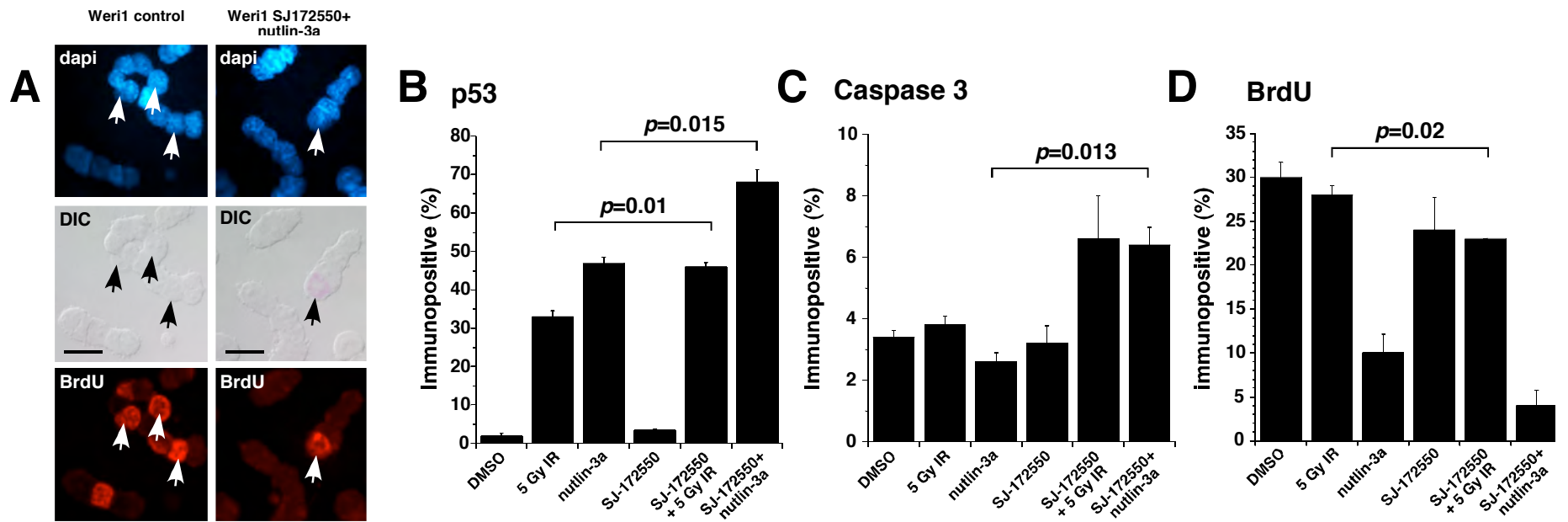


Supplemental Fig. 6. SJ-134433 and SJ-044557 are unstable and covalently modify MDMX. (A) Heat map of normalized activity for the 11 compounds selected for follow-up characterization. Dark blue is more favorable for each measurement, and the compounds are listed in order of binding constant for MdmX from best (top) to worst (bottom). These data initially suggested that SJ-134433 and SJ-044557 would be good candidates for additional biochemical studies. (B-G) High-performance liquid chromatography (HPLC-UV-MS) of each compound in FP binding buffer after incubation for 0, 2, and 24 h at room temperature. (B-D) SJ-134433 showed several contaminating peaks, and the dominant peak that is consistent with the compound's mass (box) was unstable after 2 h and completely degraded after 24 h. (E-G) SJ-044557 showed 2 isomers of the compound (boxes) and only minor contaminating species. However, after 24 h in FP buffer at room temperature, the degradation product that migrated at 2.13 had accumulated, despite the fact that a significant proportion of SJ-044557 remained. (H, I) High-resolution MALDI mass spectrometry was performed after the purified MDMX²³⁻¹¹¹ protein was incubated in the presence of each compound for 2 h in FP buffer. The shift in the mass of the MDMX²³⁻¹¹¹ protein (red vs. black line) indicated the covalent modification by SJ-134433, SJ-044557, or their byproducts.

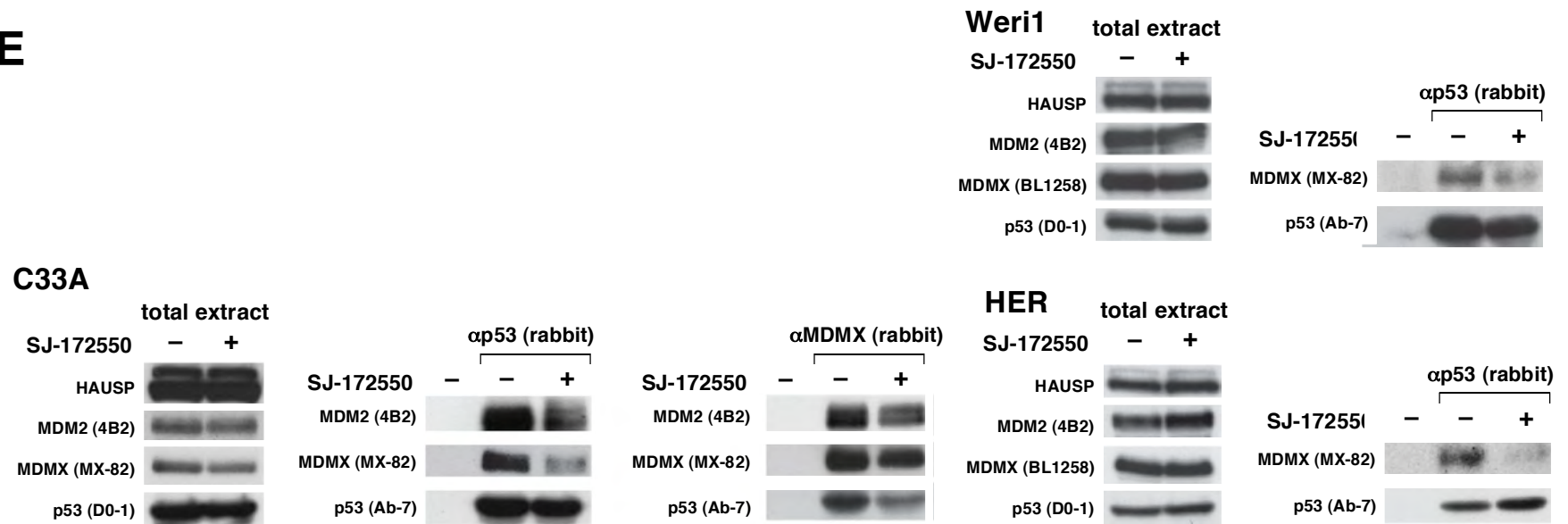


Supplemental Fig. 7.SJ-172550 cytotoxicity requires p53 (A) Representative images of Weri1 retinoblastoma cells following treatment with vehicle (DMSO- control) or SJ-172550 + nutlin-3a. The cells were labeled with BrdU for 1 hour immediately before they were fixed. Arrows indicate BrdU immunopositive cells in the red (Cy3) channel. (B-D) Histograms of the proportion of immunopositive cells for p53, activated Caspase 3 and BrdU with different treatments. Each bar represents the mean and standard deviation of scoring in triplicate of 250 cells for each condition and each antigen. Statistically significant difference are indicated. (E,F) Histogram of the proportion of p53 or activated Caspase-3 immunopositive cells following treatment with different agents as in (B-D). (E) Reciprocal immunoprecipitation showed the partial inhibition of MDMX-p53 binding in C33A, HER, and Weri1 cells. Abbreviations: DIC, differential interference contrast microscopy. Scale bars: 10 μ M.

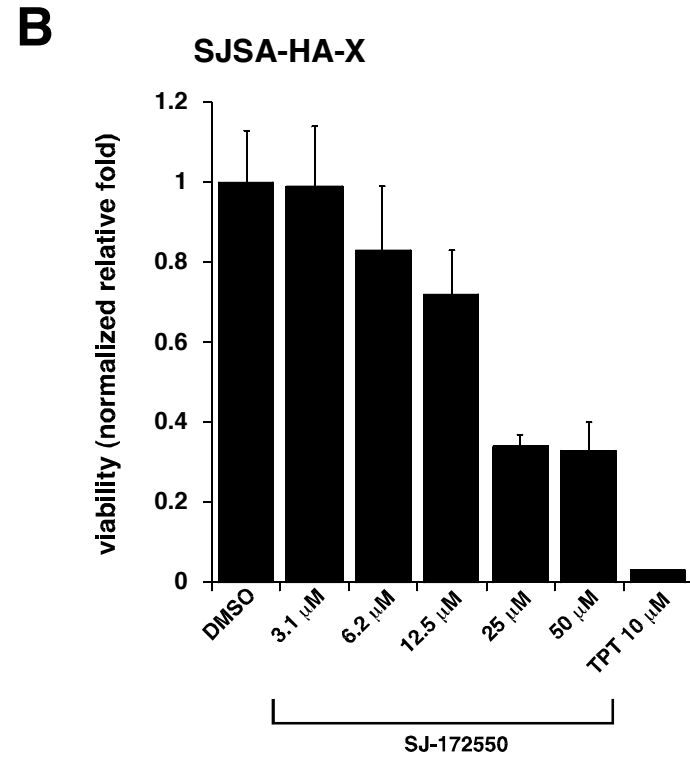
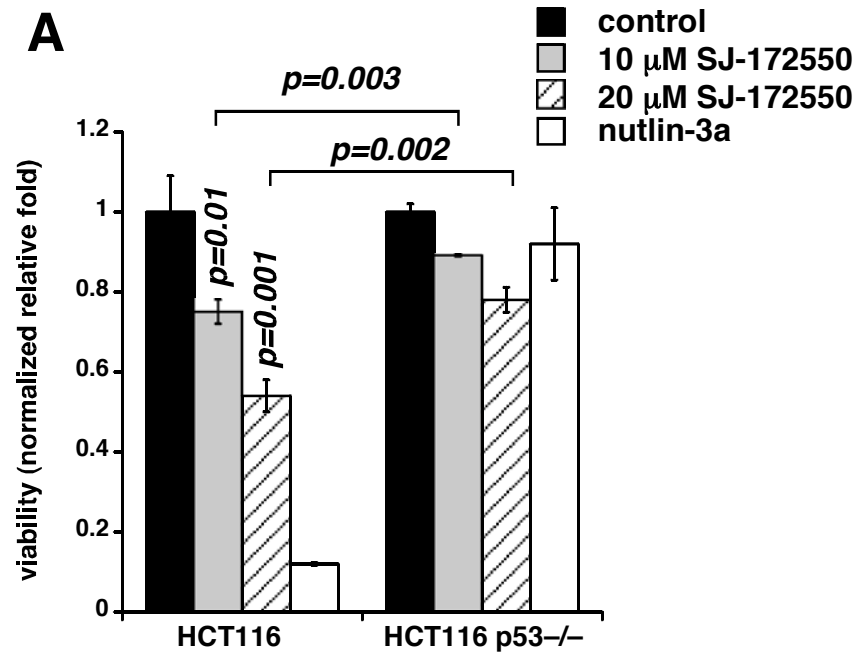
Reed et al. Sup. Fig. 7



E

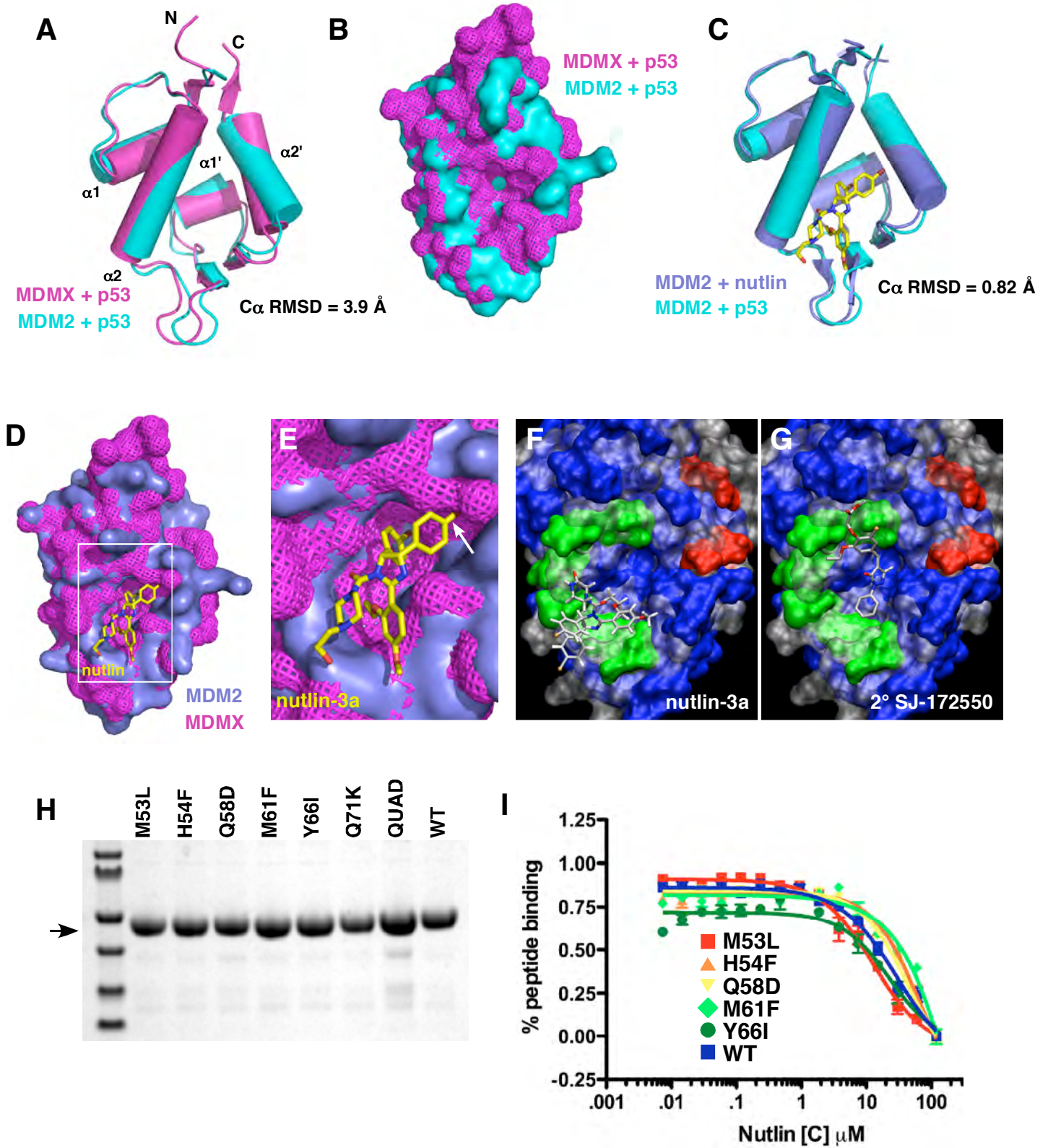


Supplemental Fig. 8. SJ-172550 cytotoxicity in cultured cells (A) Histogram of proportion of viable cells following 72 hour exposure to SJ-172550 at different concentrations. Both HCT-116 and p53-deficient HCT-116 cells were tested. Each bar represents the mean and standard deviation of triplicate samples. **(B)** Previously described SJSA-X cells expressing high levels of MDMX were tested for SJ-172550 cytotoxicity over a range of concentrations. Each bar represents the mean and standard deviation of triplicate samples exposed to SJ-172550 for 72 hours. Topotecan was used as a positive control and DMSO was used as a negative control.



Supplemental Fig. 9. Binding of SJ-172550 to MDMX mutants. (A) Alignment of the MDMX and MDM2 structures bound to p53 peptide shows some differences in the tertiary structure of the proteins; the key difference is in the angle of $\alpha 2'$. (B) A space-filling representation of the p53-binding pocket with the overlay of MDMX (pink mesh) and MDM2 (teal solid). (C) Similar alignments of nutlin-3a bound to MDM2 and the p53 peptide bound to MDM2 suggest that there is no dramatic shift in the higher-order structure when nutlin-3a is bound. (D, E) A space-filling model of the overlaid MDM2-nutlin-3a (teal) with MDMX-p53 (pink) shows that nutlin-3a binding to MDMX may be disrupted by the side chain near the outer edge of the pocket (arrow in E). (F,G) Docking of nutlin-3a and the secondary binding mode predicted for SJ-172550 to MDMX superimposed on the crystal structure of p53 peptide bound to MDM2. This mode is less favorable than that shown as the primary mode in Fig. 5D. The gray is the solvent excluded surface of MDM2 (PDB: 2Z5T) and the blue is the surface for MDMX. Green residues represent single mutations and residues shown in red formed a quadruple mutant. The first set of residues were changed to displace SJ-172550 based on the models of the most energetically favorable docking poses (Fig. 5D). These residues within MDMX were changed as follows: Q58D, M61F, Y66I and Q71D. A second series of residues were changed to make the MDMX binding pocket more like MDM2 in order to determine if SJ-172550 was binding in the p53 binding pocket. These residues include M53L, H54F and a quadruple mutant (QUAD) with P95H+S96R+P97K+R103Y. From top to bottom the green residues are M53, H54, Q58, M61, Y66 and Q71 with the red residues being R103, P97, S96 and P95. (H) Image of a coomassie stained SDS-PAGE gel of with each of the GST-MDMX mutants and a wild type control protein prepared side-by-side. Arrow indicates the recombinant GST-MDMX protein. (I) Competition experiments with each MDMX mutant and increasing concentrations of nutlin-3a. Each data point is the mean and standard deviation of triplicate assays. The proteins that did not show direct binding of p53 peptide could not be analyzed in this competition experiment.

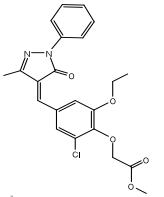
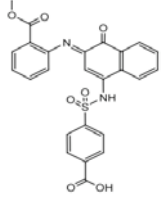
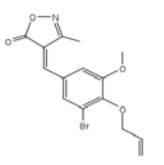
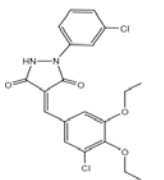
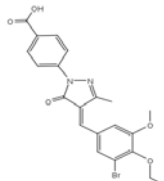
Reed et al. Sup. Fig. 9

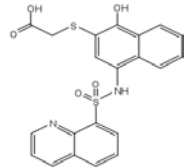
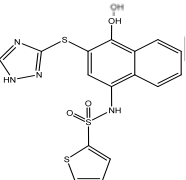
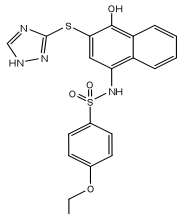
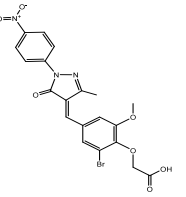
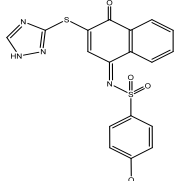
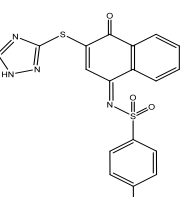


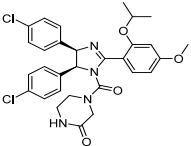
References

1. Morris, G. M., Huey, R., Lindstrom, W., Sanner, M. F., Belew, R. K., Goodsell, D. S., and Olson, A. J. (2009) *J Comput Chem* **30**, 2785-2791.

Supplemental Table 1. Summary of Selected Validated Hits from MDMX High-Throughput Screening

Number (cluster)	MW	Structure	¹ Stability DMSO	² Stability FP (2/24 hr)	³ Protein Conjugate	Solubility (μM)	Permeability (10 ⁻⁶ cm/s)	⁴ MDMX EC ₅₀ (μM)	⁴ MDM2 EC ₅₀ (μM)	Δmp (°C)	⁵ Redox (%)	⁴ Weri1 EC ₅₀ (μM)	⁴ Rbl-8 EC ₅₀ (μM)	⁴ BJ EC ₅₀ (μM)
172550 (1)	428.87		Yes	Yes/Yes	No	6.2	12.86	2.3±0.3	26.0±15.4	8.3	None	23.1±4.4	24.0±11.9	>50
44557 (54)	490.48		Yes	Yes/Yes	Yes	31.9	47.06	0.32±0.6	0.21±0.3	-1.4	Med	4.2±0.8	9.0±1.4	>50
34877 (7)	352.18		No	Yes/Yes	No	<0.28	0	8.3±0.5	14.8±0.4	11.4	None	29.6±43.1	10.5±6.2	>50
165217 (1)	421.27		Yes	Yes/No	No	<0.24	0	5.56±3.1	5.2±2.05	9.3	None	10.5±1.9	8.4±2.9	>50
158964 (4)	459.29		Yes	Yes/No	No	<0.22	37.68	2.8±0.7	2.2±1.5	9.1	Low	25.9±8.6	13.6±14.8	>50

135056 (8)	440.49		Yes	Yes/No	Yes	65.3	9	0.26±0.13	0.78±0.83	-2.9	High	5.4±1.0	4.8±0.7	24-30
134433 (11)	404.49		No	No/No	Yes	63.4	0.12	0.12±0.15	0.34±0.18	-1.9	Low	4.4±1.0	5.3±0.8	26
247100 (11)	442.51		Yes	No/No	No	44	0	8.5±6.6	8.1±6.5	8	Med	5.2±1.1	3.4±1.1	24
185452 (4)	490.26		Yes	Yes/No	No	48.8	6.01	1.9±1.5	2.3±0.9	10.6	114	>50	35.5±133	>50
44512 (5)	426.47		No	Yes/Yes	Yes	19.5	2.0	0.25±0.25	0.27±0.33	n.d.	n.d.	3.6±0.8	3.6±0.5	2.3
44509 (5)	430.89		No	Yes/Yes	Yes	24.3	15.9	0.24±0.15	0.28±0.23	-1.4	70.7	3.7±0.8	4.8±0.9	14-20

Nutlin3a	581.49		n.d.	n.d.	n.d.	66.9	1382	26.5±0.6	0.68±0.06	-2	n.d.	2.3±0.6	33.4±15.8	n.d.
----------	--------	---	------	------	------	------	------	----------	-----------	----	------	---------	-----------	------

¹ Compounds were dissolved in DMSO and analyzed by MS 2 hours later.

² Compounds were dissolved in the fluorescence polarization (FP) buffer used for the HTS and analyzed 2 and 24 hours later.

³ Covalent protein modification from each compound was analyzed using MS after a 2 hour incubation in FP buffer.

⁴ All values are the mean of triplicate experiments with standard deviation.

⁵ The redox classifications were set across 3 equally spaced bins of the active dataset. The active dataset was selected using robust statistics with RISE with outlier from negative controls being required and no percent activity cutoff. The high group was greater than 75% active, the mid group was 40-75% active, the low group was 20-40% active and the inactive compounds were less than 20% active.